Anisotropic Spin-Disorder Resistivity of AuMn†

W. BINDLOSS*
Department of Physics, University of California, Berkeley, California
(Received 20 March 1967; revised manuscript received 22 August 1967)

The results of measurements of the a-axis and c-axis resistivity of a single crystal of the planar antiferromagnet AuMn are reported for the temperature range 4.2–560°K. The resistivity of this material rises rapidly with increasing temperature in the antiferromagnetic region, reaching a value of 61 $\mu\Omega$ cm at the Néel temperature of 500°K. Above this temperature, the resistivity increases linearly with temperature, but with a smaller slope which is determined by the lattice resistivity. The single-crystal measurements show a significant anisotropy in the resistivity which is dependent on the state of the spin system. The temperature dependence and the anisotropy of the resistivity are analyzed, taking into account the effects of superzone boundaries associated with the spin ordering and also the presence of an anisotropic spin-disorder contribution. The superzone boundaries introduce a relatively small anisotropy into the resistivity ($\approx 8\%$ at $T=4.2$°K) such that $\rho_c > \rho_a$, while the spin-disorder resistivity contributes a much larger anisotropy of the opposite sign in the temperature region 200–500°K. A simplified model of the AuMn magnetic lattice is used to calculate the spin-wave contribution to the low-temperature resistivity using a one-band model for the conduction electrons. This calculation is in good agreement with the magnitude and anisotropy of the low-temperature resistivity. The spin-disorder resistivity is also treated using the quasielastic approximation with the effects of correlation in the spin fluctuations included. It is found that the magnitude and form of the spin correlations can be directly related to the spin-disorder resistivity as a function of crystallographic direction. The anisotropy of the spin-disorder resistivity observed in AuMn is discussed in terms of anisotropic spin correlations for the temperature range $0.7T_N < T < T_N$.

I. INTRODUCTION

THE electrical resistivity of ferromagnetic and antiferromagnetic metals has been the subject of a number of experimental and theoretical investigations. The resistivities of the ferromagnetic transition metals,[1] of the heavy rare-earth metals,[2] and of a variety of intermetallic compounds[3–5] exhibiting magnetic transitions have been measured over the range of temperature in which magnetic ordering takes place. In these materials, one observes a significant contribution to the resistivity which is dependent on the magnetic state of the system. However, the quantitative interpretation of such resistivity data is often difficult because of the complicated electronic-band structures of these materials. In both the rare-earth and the 3-d transition metals, there is a large contribution to the density of states at the Fermi energy from electrons of predominantly d symmetry, so that s-d interband transitions play an important role in determining the transport properties. The interpretation of the spin-disorder resistivity of the heavy rare-earth metals is further complicated by their noncubic lattice symmetry and complex spiral and helical magnetic structures. In this paper, a detailed investigation is presented of the spin-disorder resistivity of the antiferromagnetic compound AuMn. This compound is a particularly simple one for study, because it has a two-sublattice antiferromagnetic structure below 500°K, a lattice symmetry which is close to simple-cubic, and because the contribution of d electrons to the density of states at the Fermi energy is unusually small.

Several authors[6–9] have investigated the spin-disorder resistivity of magnetic metals using a spin-dependent interaction of the form

$$H = -2G\delta(\mathbf{R}_n - \mathbf{r})\,\mathbf{S}_n \cdot \mathbf{s}. \tag{1}$$

Equation (1) describes the interaction between a conduction electron at $\mathbf{r}$ with spin $\mathbf{s}$ and a localized magnetic moment at $\mathbf{R}_n$ with spin $\mathbf{S}_n$. For a completely disordered spin system, Eq. (1) leads to a spin-disorder resistivity

$$\rho^M = (3\pi N m/2\hbar e^2)\,(G^2/E_F)\,S(S+1). \tag{2}$$

The quantity N is the number of localized magnetic spins per unit volume. Eq. (2) is satisfied by the heavy rare-earth metals in the disordered state using values for G of the same order of magnitude as required to explain the exchange interactions through the Ruderman-Kittel-Kasuya-Yosida[10–12] RKKY mechanism. The contribution to the resistivity arising from

† Supported by the U.S. Atomic Energy Commission through Contract No. AT (11-1)-34, Project 47. Report Code UCB-34P47-4.
* Present address: Central Research Department, E.I. du Pont de Nemours and Company, Wilmington, Delaware.
[1] G. K. White and S. B. Woods, Phil. Trans. Roy. Soc. London **A251**, 273 (1958).
[2] R. V. Colvin, S. Leggvold, and F. H. Spedding, Phys. Rev. **120**, 741 (1960).
[3] P. E. Bierstedt, Phys. Rev. **132**, 669 (1963).
[4] Chang-Chih Chao, J. Appl. Phys. **37**, 2081 (1966).
[5] A. Giansoldati, J. O. Linde, and G. Borelius, J. Phys. Chem. Solids **11**, 46 (1959).
[6] K. Yosida, Phys. Rev. **107**, 396 (1957).
[7] T. van Peski-Tinbergen and A. J. Dekker, Physica **29**, 917 (1963).
[8] T. Kasuya, Progr. Theoret. Phys. (Kyoto) **16**, 58 (1956); **22**, 227 (1959).
[9] P. G. de Gennes and J. Friedel, J. Phys. Chem. Solids **4**, 71 (1958).
[10] M. A. Ruderman and C. Kittel, Phys. Rev. **96**, 99 (1954); T. Kasuya, Progr. Theoret. Phys. (Kyoto) **16**, 45 (1956); K. Yosida, Phys. Rev. **106**, 893 (1957).
[11] P. G. de Gennes, J. Phys. Radium **23**, 510 (1962).
[12] Y. A. Rocher, Phil. Mag. Suppl. **11**, 223 (1962).

spin-wave–electron scattering has been calculated by Kasuya[8] using a single-band approximation. In the case of Gd, the single-band theory predicts a resistivity which is two orders of magnitude too small in the temperature region above 40°K for any reasonable values of G.[13] Goodings[14] has extended the spin-wave treatment to include the possibility of s-d interband transitions. For the spin-disorder resistivity of Gd he predicts a resistivity which has a predominantly linear form above 40°K, and which is of the right order of magnitude in comparison with experimental measurements. A two-band theory is also required in the case of the ferromagnetic 3-d transition metals.[14,15]

A number of authors[16] have discussed the problem of the localization of a magnetic state in a metal. For dilute alloys of Mn with Cu, Ag, and Au, the localized magnetic state has been described as a virtual bound state within the host metal conduction band. The transport cross section of such a state must be assumed to contain both a spin-dependent and a spin-independent part, both of which will contribute to the resistivity in a dilute alloy. However, for the chemically ordered AuMn alloy discussed here, the spin-independent part of the conduction-electron–local-moment interaction will not contribute to the spin-disorder resistivity because of the Bloch theorem. We shall assume here that the spin-dependent part of the interaction can be represented adequately by Eq. (1). Since the localized magnetic state contributes a d-electron density of states at the Fermi energy, one must consider the influence of s-d interband transitions. In the analysis of the results presented here, a one-band model will be used. The justifications for the use of this simplified model are presented in Sec. II, along with a discussion of the magnetic and electronic properties of the AuMn lattice. We will find in Secs. IV and V that both the magnitude of the low-temperature resistivity and the anisotropy in the resistivity observed at higher temperature can be accounted for semiquantitatively in terms of a one-band free-electron model.

II. MAGNETIC AND ELECTRONIC PROPERTIES OF AuMn

The magnetic and crystallographic structure of the AuMn compound has been investigated by neutron diffraction,[17] x-ray,[18] and torsion[19] studies. The alloy crystallizes in the simple cubic, *ordered*, CsCl structure over a broad range of concentration around 50 at.% Au. For concentrations within a few percent of ideal stoichiometry (AuMn), the crystal transforms at about 500°K to the two-sublattice antiferromagnetic structure shown in Fig. 1. This transformation is accompanied by a martensitic transformation to a tetragonal lattice with $c/a=0.97$ (t_1 phase). For alloys with Au concentrations of less than 51 at.%, a second transformation occurs at a somewhat lower temperature to a different crystallographic phase having a more complicated magnetic structure.[17] This second transformation is inhibited for bulk samples with Au concentrations in excess of 51 at.%. The single crystal discussed here was found to be 51.5 at.% Au by chemical analysis, and showed no evidence of a $t_1 \rightarrow t_2$ transformation over a period in excess of two years.

The susceptibility[20] and electrical resistivity[21] of polycrystalline AuMn in the t_1 phase have been measured over a broad range of temperature up to 1000°K. The susceptibility has the usual form associated with a simple two-sublattice antiferromagnet. From the susceptibility in the paramagnetic region, one obtains a paramagnetic Curie temperature Θ_p of -280°K, and a magnetic moment of 4.8 μ_B per Mn ion.[5] Neutron-diffraction measurements[17] give a magnetic moment of between 4.0 and 4.2 μ_B per Mn ion for this material, which is in substantial disagreement with the above estimate. These values were obtained without considering important contributions due to the spin-polarization of conduction electrons in the vicinity of the magnetic ion,[11] and thus should not be directly equated with the magnetic moment associated with the manganese d states. In the case of AuMn, a further complication is involved. The interpretation of torsion measurements[19] indicated that the sublattice magnetization was locally pinned at random sites throughout the crystal. It is possible that the magnetization may be pinned in directions out of the aa plane at some of these pinning sites. This kind of pinning would cause a reduction of the intensity of the magnetic reflections observed in

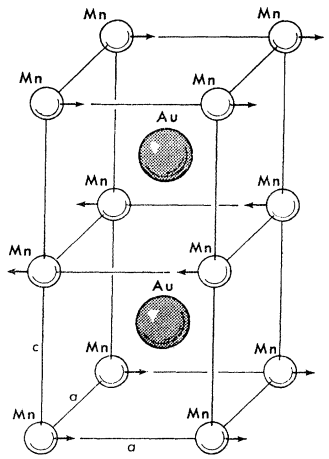

FIG. 1. The magnetic structure of the t_1 phase of AuMn.

[13] D. A. Goodlings, J. Appl. Phys. **34**, 1370 (1963).
[14] D. A. Goodlings, Phys. Rev. **132**, 542 (1963).
[15] A. Hasegawa, S. Wakoh, and J. Yamashita, J. Phys. Soc. Japan **20**, 1865 (1965).
[16] J. Friedel, Nuovo Cimento Suppl. **7**, 287 (1958); A. Blandin and J. Friedel, J. Phys. Radium **20**, 160 (1959); P. W. Anderson, Phys. Rev. **124**, 41 (1961); P. A. Wolff, *ibid.* **124**, 1030 (1961); J. R. Schrieffer and D. C. Mattis, *ibid.* **140**, A1412 (1965); B. Kjöllerstrom, D. J. Scalapino, and J. R. Schrieffer, *ibid.* **148**, 665 (1966).
[17] E. E. Bacon, Proc. Phys. Soc. (London) **79**, 938 (1961).
[18] J. H. Smith and P. Gaunt, Acta Met. **9**, 819 (1961).
[19] W. Bindloss, J. Phys. Chem. Solids (to be published).
[20] A. Gainsoldati, J. Phys. Radium **16**, 342 (1955).
[21] A. Gainsoldati and J. O. Linde, J. Phys. Radium **16**, 341 (1955).

neutron-diffraction measurements, resulting in a low estimate for the magnetic moment.

According to the usual description of a localized magnetic state,[16] a magnetic moment substantially less than 5 μ_B per Mn ion would result in a large d-electron contribution to the density of states at the Fermi energy. Measurements of the electronic specific heat[22] of the AuMn compound give a density of states at the Fermi energy of 0.445 el./eV atom. Comparing this result with the values for γ Mn (3.9 el./eV atom),[23] 50 at.% CuMn ($\approx$2.5 el./eV atom),[24] and the ferromagnetic 3-d transition metals ($\approx$2 to 3 el./eV atom),[25] it is apparent that the large d-state contribution which is usually observed is not present in the AuMn compound. The value 0.445 el./eV atom is in fact only 49% larger than the free-electron value for the case of Mn^{+} $^{+}Au^{+}$ ions (1.5 el./atom). Since we can expect an enhancement of the free-electron specific heat of 20% or more due to electron-phonon interactions,[26] we conclude that the d-electron contribution is a relatively small percentage of the total Fermi-level density of states. This result suggests that the magnetic moment per Mn ion may be close to 5 μ_B. Thus, on the basis of the specific-heat result, we shall assume a nearly free-electron approximation based on Mn^{+} $^{+}Au^{+}$ ion cores and a spin-$\frac{5}{2}$ state for the Mn^{+} $^{+}$ ion. The most important consequence of this assumption is that the effects on the spin-disorder resistivity of magnon-induced s-d interband transitions are neglected. These transitions result in an enhancement of the spin-disorder resistivity at temperatures large enough to excite magnons whose wave vectors span the distance between s- and d-electron Fermi surfaces.[14] However, since the d-electron-state density is small, the one-band model is considered to be a reasonable first approximation for this material.

The validity of a one-band model can also be examined in the light of the lattice resistivity, since phonon-induced interband transitions enhance the lattice resistivity in the same manner that magnon-induced transitions enhance the spin-disorder resistivity. Let us characterize the magnitude of the lattice resistivity by the dimensionless parameter[27]

$$R=(4e^2mk_B\Theta_D{}^2/\pi^3\hbar^3 2^{-1/3}Q_mT)\rho_L,$$

which is approximately the ratio of the measured lattice resistivity ρ_L to the theoretical lattice resistivity given by the Bloch formula for a one-band, free-electron metal. One finds that for most of the nontransition metals R varies between 1 and 4. On the other hand, for the 3-d, 4-d, and 5-d transition metals R varies between approximately 10 and 60, indicating that for these materials a substantial enhancement is present. Using the estimate of the lattice resistivity of AuMn obtained in Sec. III, we find $R\approx3.5$. This value, by comparison with those above, suggests that interband transitions do not greatly enhance the phonon resistivity of AuMn, and correspondingly that a reasonable first approximation to the spin-disorder resistivity can be obtained using a one-band model.

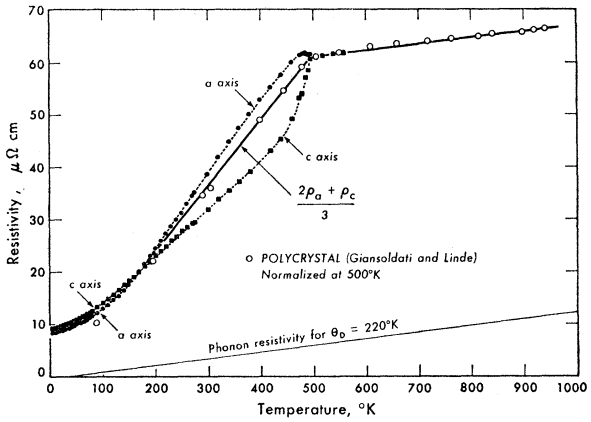

FIG. 2. The a-axis and c-axis resistivities of AuMn versus temperature.

III. EXPERIMENTAL RESULTS

The procedure used in the growth of the single crystal, and its analysis by x-ray and torsion studies has been described in detail elsewhere.[19] Two resistivity samples, with cross-section 1×1 mm and length 5 mm, were spark-cut from a finely-twinned crystal containing two twin orientations sharing a common a-axis. In the a-axis sample, both twins share a common a axis which is directed along the length of the sample. In the c-axis sample, the c axis of the predominant twin is directed along the length of the sample. The volume ratio of the two twin orientations in the c-axis sample was found to be 3:1 by torsion measurements.

Resistivity measurements were made using a four-probe device with current and potential probes spring-loaded against the sample. The potential probes, which were separated by approximately 2 mm, were cemented into a Bakelite block, and the entire block was spring-loaded against the sample so that the probe separation was reproducible. The temperature of the sample was measured by a calibrated copper-constantan thermocouple which was glued directly to the surface of the sample.

In Fig. 2, the measured a-axis and c-axis resistivities are plotted versus temperature. The c-axis resistivity was computed using the measured twin ratio of the c-axis sample. The data of Gainsoldati and Linde[21] on polycrystalline AuMn have been normalized to agree

[22] J. C. Ho and W. Bindloss, Phys. Letters **20,** 459 (1966). The value for the Fermi level density of states is incorrectly reported. The correct value is 0.445 el./eV atom; thus the ratio of the measured density of states to the free-electron density of states is 1.49.
[23] J. C. Ho and N. E. Phillips, Phys. Letters **10,** 34 (1964).
[24] J. E. Zimmerman and H. Sato, J. Phys. Chem. Solids **21,** 71 (1961); J. C. Ho, thesis, University of California, Berkeley, 1956 (unpublished).
[25] C. Kittel, *Introduction to Solid State Physics* (John Wiley & Sons, Inc., New York, 1966), p. 212.
[26] N. W. Ashcroft and J. W. Wilkins, Phys. Letters **14,** 285 (1965).
[27] J. M. Ziman, *Electrons and Phonons* (Clarendon Press, Oxford, England, 1960).

with the data of Fig. 2 at 500°K, and are plotted in Fig. 2 along with the computed polycrystalline resistivity for comparison. Also shown in Fig. 2 is an estimate of the phonon contribution to the resistivity. The absolute magnitude of these resistivity measurements may be in error by as much as 10% because of the difficulty in measuring sample size and probe separation accurately. However, the relative magnitude of the c-axis and a-axis resistivities is considered to be accurate within 5% error since the two sets of data were normalized to agree for $T>T_N$, where the crystal is cubic. The two samples used are considered to be equivalent since they were cut from the same cross section of a single crystal.

Analysis of Results

Assuming that the phonon contribution to the resistivity is linear above 500°K, the linearity of the resistivity-versus-temperature curve above 500°K indicates that the spin-disorder resistivity is independent of temperature in the paramagnetic region. Deviations from a constant spin-disorder resistivity in the paramagnetic region arising from temperature-dependent spin correlations have been examined theoretically by deGennes and Friedel[9] in terms of the parameter k_Fd, where d is a nearest-neighbor distance. Their results show that the deviations should be negligible for $k_Fd\gtrsim 4$. The condition $k_Fd\gtrsim 4$ is satisfied by the AuMn crystal for either singly or doubly valent Mn ion cores.

The phonon contribution to the resistivity shown in Fig. 2 was estimated using the slope of the resistivity-versus-temperature curve in the paramagnetic region, and using the Grüneisen-Bloch formula for the lattice resistivity. The Debye temperature chosen is that of Au multiplied by the square root of the density ratio ρ_{Au}/ρ_{AuMn}. Subtracting the lattice and residual contributions from the total resistivity above $T=T_N$, we obtain $\rho^M=47$ $\mu\Omega$ cm for the spin-disorder resistivity in the paramagnetic region. Assuming $Mn^{+}+Au^{+}$ ion cores and $S=\frac{5}{2}$, we find from Eq. (2) that $G=7.2$ eV Å^3. The parameter $J(0)$ used by Yosida[10] is given by $J(0)=G/\Omega=0.44$ eV, where Ω is the atomic volume. The sign of the constant G is not determined. The large residual resistivity shown in Fig. 2 is to be expected because of the disorder associated with the deviation of 1.5 at.% from ideal stoichiometry.

Since the lattice is nearly cubic below 500°K, we shall assume that the anisotropy of the resistivity below 500°K may be attributed to the presence of the planar magnetic ordering and the associated spin-wave excitations. For a conduction-electron–local-moment interaction of the form (1), the planar magnetic ordering of the Mn spins gives rise to a set of new band gaps,[28,29] of magnitude $\Delta\approx NG\langle S\rangle\approx 0.5$ eV at superzone boundaries bisecting the vectors $\mathbf{G}\pm\mathbf{Q}$ in reciprocal space. The vector $\mathbf{G}$ is a reciprocal lattice vector, and the wave vector $\mathbf{Q}=(0,0,1)\pi/c$ characterizes the spin ordering. In the presence of these gaps, the cubic symmetry of the Fermi surface is destroyed, resulting in anisotropic transport properties. The quantitative effect is expected to be small, however, unless the superzone boundary is close to tangent to the original Fermi surface, since it is only in this case that a large reduction in Fermi-surface area occurs. The two types of superzone boundaries which affect the AuMn Fermi surface are shown in Fig. 3. This is a drawing of the nearly free-electron Fermi surface for the case of $Mn^{+}+Au^{+}$ ion cores. The free-electron Fermi surface for this case just touches the boundaries of the second zone. The boundaries of the cubic first B.Z. and the associated band-gaps have been suppressed in the drawing since the zone is full except for a small pocket of holes in the (1, 1, 1) corners.

Assuming that the impurity scattering is isotropic, we may attribute the anisotropy observed in the residual resistivity to the distortion of the Fermi surface resulting from the superzone boundaries. Thus we conclude that the superzone boundaries introduce a relatively small ($\approx 8\%$) anisotropy in the resistivity at $T=0$, and such that $\rho_c(0)>\rho_a(0)$. The large anisotropy in the resistivity observed between 200 and 500°K, which has the opposite sign, will therefore be attributed to the spin-disorder contribution ρ^M. In order to estimate the spin-disorder contribution we shall make use of the results of Elliott and Wedgwood.[28] For a single superzone boundary which cuts the Fermi surface into two parts, and which bisects the vector $\mathbf{G}\pm\mathbf{Q}=2\mathbf{l}$, they find for the resistivity measured in the direction of $\mathbf{l}$:

$$\rho(T)=[\rho^R+\rho^L(T)+\rho^M(T)]/[1-\delta(T)]. \quad (3)$$

Here ρ^R, $\rho^L(T)$, and $\rho^M(T)$ are the residual, phonon, and spin-disorder contributions to the resistivity in the absence of the magnetic band gap, and $\delta(T)=(3\pi l/4k_F)(\Delta/E_F)$. For AuMn, we have $\Delta/E_F\approx 0.07$ at

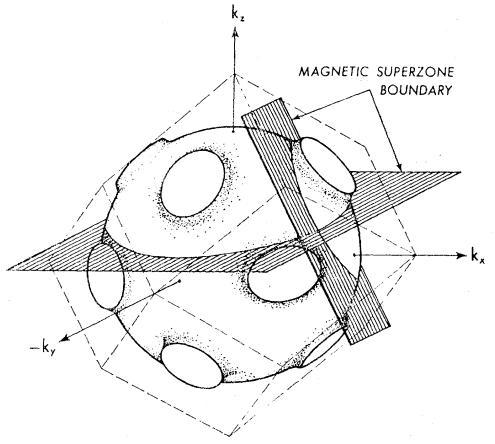

FIG. 3. Nearly free-electron Fermi surface of AuMn in the extended zone scheme, with representative magnetic superzone boundaries included. The boundaries of the first Brillouin zone have been suppressed.

[28] R. J. Elliot and F. A. Wedgwood, Proc. Phys. Soc. (London) **81**, 846 (1963).
[29] A. J. Freeman, J. O. Dimmoch, and R. E. Watson, Phys. Rev. Letters **16**, 94 (1966).

$T=0$. Guided by the form of Eq. (3), we shall express the resistivity in the form

$$\rho_a(T)=[\rho^R+\rho^L(T)+\rho_a{}^M(T)]/[1-\delta_a(T)], \quad (4)$$

and

$$\rho_c(T)=[\rho^R+\rho^L(T)+\rho_c{}^M(T)]/[1-\delta_c(T)], \quad (5)$$

where $\rho_a{}^M(T)$ and $\rho_c{}^M(T)$ are the spin-disorder resistivities measured in the a and c directions. The quantities $\delta_a(T)$ and $\delta_c(T)$ have the temperature dependence of the sublattice magnetization. The measured resistivity at $T=4.2°$K allows the unique determination of only two of the unknown parameters $\delta_a(0)$, $\delta_c(0)$, and ρ^R. However, we can obtain the correct sign for the anisotropy $\rho_a{}^M(T)-\rho_c{}^M(T)$ if we assume that $\delta_a(0)=0$ and evaluate $\delta_c(0)$ and ρ^R from the measured resistivity at $T=4.2°$K. Figure 4 shows the spin-disorder resistivity computed by this procedure with $\delta_c(T)$ fitted to a Brillouin function for $S=\frac{5}{2}$. The magnitudes of $\rho_a{}^M(T)$ and $\rho_c{}^M(T)$ shown in Fig. 4 should be considered only as rough approximations. Figure 4 also contains the result of a spin-wave calculation which is discussed in Sec. IV.

IV. SPIN-WAVE THEORY

In this section we shall analyze the spin-wave spectrum and the electron-magnon interaction of the AuMn structure, and present the results of a calculation of the contribution of magnon-electron scattering to the electrical resistivity. To calculate the spin-wave spectrum one should, ideally, have a theory which is capable of predicting the exchange constants between ions at arbitrarily large distances. However, estimates which have been made[30] of the Néel temperature and paramagnetic Curie temperature using RKKY[10–12] and virtual state theories[31] do not give results accurate enough to justify their use in determining the spin-wave spectrum. The approach taken here is to use the simplest model for the exchange interactions consistent with the stability of the spin structure, and to evaluate the exchange constants empirically using the measured values for T_N and Θ_p. We shall see that all of the important features of the spin-wave spectrum are properties of the symmetry of the system. Thus, since the maximum spin-wave energy for a given Néel temperature is relatively independent of the range of the exchange interactions, we should obtain a reasonable first approximation to the excitation spectrum.

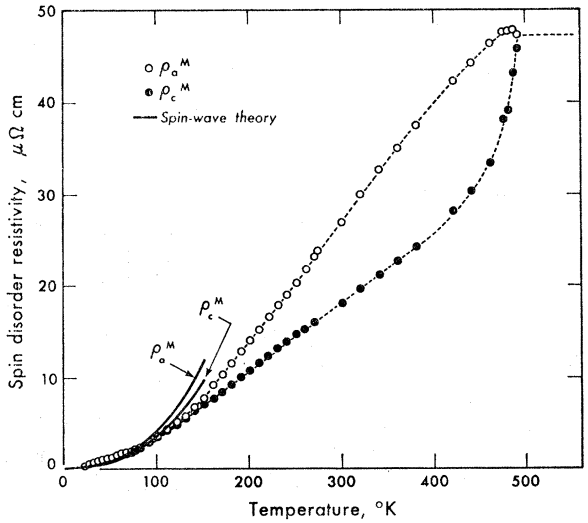

FIG. 4. The a-axis and c-axis spin-disorder resistivities of AuMn versus temperature.

We shall now adopt a model which includes only first- and second-nearest-neighbor exchange. We shall also neglect the slight tetragonal distortion of the lattice and assume that the exchange interactions have cubic symmetry. The deviation from cubic symmetry given by current theories[10–12,31] of the indirect exchange interaction are small for the first few neighbor shells. The stability of the AuMn spin structure requires that the first-nearest-neighbor exchange J_1 be ferromagnetic, that the second-nearest-neighbor exchange J_2 be antiferromagnetic, and that $4|J_2|>|J_1|$.[32] Introducing a small anisotropy field H_A to stabilize the array, the Hamiltonian is

$$H=-\sum_{i\delta} J_{i\delta}\mathbf{S}_i\cdot\mathbf{S}_\delta+2\mu_B H_A[\sum_\beta S_\beta{}^\zeta-\sum_j S_j{}^\zeta]. \quad (6)$$

The quantity $\mathbf{S}_\delta$ denotes a spin which is a first or second neighbor to the spin $\mathbf{S}_i$, and the ζ direction is defined as the axis of quantization, which is an a axis. The indices j and β denote sites on the up and down sublattices, respectively. Adopting the convention that J_1 and J_2 be positive, then $J_{i\delta}=J_1$ for $\delta=$1st-nearest neighbors, and $J_{i\delta}=-J_2$ for $\delta=$2nd-nearest neighbors. Using the Holstein–Primakoff[33] transformation to the spin-wave variables

$$a_\mathbf{q}=(NS)^{-1/2}\sum_j \exp(i\mathbf{q}\cdot\mathbf{R}_j)S_j{}^+,$$

$$b_\mathbf{q}=(NS)^{-1/2}\sum_\beta \exp(-i\mathbf{q}\cdot\mathbf{R}_\beta)S_\beta{}^-, \quad (7)$$

and diagonalizing the Hamiltonian through the transformation to normal-mode spin-wave variables

$$\alpha_\mathbf{q}=u_\mathbf{q}a_\mathbf{q}-v_\mathbf{q}b_\mathbf{q}{}^\dagger, \qquad \beta_\mathbf{q}=u_\mathbf{q}b_\mathbf{q}-v_\mathbf{q}a_\mathbf{q}{}^\dagger, \quad (8)$$

one obtains the following expression for the spin-wave energy:

$$E(\mathbf{q})=(A_\mathbf{q}{}^2-B_\mathbf{q}{}^2)^{1/2}, \quad (9)$$

where

$$A_\mathbf{q}=2S[4J_2(1+c_xc_y)-2J_1(c_x+c_y-1)]+\omega_A,$$

$$B_\mathbf{q}=2S[4J_2(c_xc_z+c_yc_z)-2J_1c_z], \quad (10)$$

[30] W. Bindloss, thesis, University of California, Berkeley, 1967 (unpublished). Available from University microfilms, 300 Zeeb Road, Ann Arbor, Mich.

[31] B. Caroli and A. Blandin, J. Phys. Chem. Solids **27**, 503 (1966); B. Caroli, *ibid.* **28**, 1427 (1967).

[32] R. A. Tahir-Kheli, H. B. Callen, and H. Jarrett, J. Phys. Chem. Solids **27**, 23 (1966).

[33] T. Holstein and H. Primakoff, Phys. Rev. **58**, 1098 (1940).

and the spectrum is doubly degenerate. The quantity ω_A is given by $\omega_A=2\mu_B H_A$, and $c_x=\cos q_x a$, etc.

Within the first magnetic Brillouin zone, which is tetragonal with $c/a=\frac{1}{2}$, the dispersion relation (9) has relative minima at the points $(0,0,0)$, $\pm(1,0,0)\pi/a$, and $\pm(0,1,0)\pi/a$. In the limit as $H_A\to 0$, the spin-wave energy becomes zero at each of these points. The existence of minima in the energy at the latter two points (we will denote these points by $\mathbf{q}_0$) on the faces of the zone is a result of the assumption of cubic symmetry for the exchange constant J_{ij}, and is independent of the range of the exchange interactions.[30] The energy gaps at the points $\mathbf{q}=0$ and $\mathbf{q}=\mathbf{q}_0$ are given by $E(0)=[8S(4J_2-J_1)\omega_A]^{1/2}$, and $E(\mathbf{q}_0)=[8SJ_1\omega_A]^{1/2}$. In the vicinity of these points, the surfaces of constant energy form ellipsoids. Using expressions for T_N and Θ_p derived from molecular-field theory, we find $J_1/k_B=17°\text{K}$, and $(4J_2-J_1)/k_B=33°\text{K}$. The magnitude of $4J_2-J_1$ can also be related to the perpendicular susceptibility, with the result $\chi_\perp=N\mu_B^2/2(4J_2-J_1)=2.8\times10^{-4}$. This value for $\chi_\perp$ is of the right order of magnitude when compared with the measured susceptibility at the Néel temperature,[20] $\chi(T_N)=2.5\times10^{-4}$, and with the susceptibility difference at room temperature,[19] $\chi_\perp-\chi_{||}\approx 9.5\times10^{-5}$. Tahir-Kheli, Callen, and Jarrett[32] have computed T_N for the AuMn structure as a function of J_1 and J_2 using a Green's function "random-phase" approximation. Their results predict exchange constants approximately twice as large as the above estimates. We shall assume here that $J_1/k_B=(4J_2-J_1)/k_B\approx 30°\text{K}$. Thus the ellipsoidal energy surfaces are approximated by spheres, which is of little consequence since the principal source of anisotropy in the resistivity is found to be the geometry associated with umklapp processes. Assuming an anisotropy field of the order of 10^4 Oe,[19] we find that the minimum excitation energy is given by $E_m/k_B\approx 30°\text{K}$. Since we are primarily interested in the resistivity for temperatures above 30°K, we will simplify further by making the assumption that $H_A=0$. Then the excitation spectrum in the vicinity of the point $\mathbf{q}=(0,0,0)$ has the form

$$E(\mathbf{q})=4SJ_1aq. \tag{11}$$

In the vicinity of the points $\mathbf{q}_0$, the excitation spectrum has the identical form when the variable $\mathbf{q}'=\mathbf{q}-\mathbf{q}_0$ is substituted for $\mathbf{q}$. The linear dependence on wave vector is a property of the two-sublattice structure, and thus is independent of the particular model used for the exchange interactions.

Electron-Magnon Interaction

Using the second quantized form for the conduction electron-localized spin interaction,[6] and transforming to magnon variables using the inverse of Eqs. (7) and (8), we obtain the following expression for the magnon-electron Hamiltonian:

$$H'=(SN)^{1/2}\sum_{\mathbf{k},\mathbf{k}',\mathbf{q}}(u_\mathbf{q}+v_\mathbf{q})\times G[(\alpha_\mathbf{q}+\beta_\mathbf{q}^\dagger)C_{\mathbf{k}'\downarrow}^\dagger C_{\mathbf{k}\uparrow}\delta(\mathbf{k}-\mathbf{k}'-\mathbf{q}+\boldsymbol{\tau})+(\alpha_\mathbf{q}^\dagger+\beta_\mathbf{q})C_{\mathbf{k}'\uparrow}^\dagger C_{\mathbf{k}\downarrow}\delta(\mathbf{k}-\mathbf{k}'+\mathbf{q}+\boldsymbol{\tau})]. \tag{12}$$

Terms describing the interaction between the conduction electrons and the long-range order of the magnetic system have been dropped, since this interaction has already been accounted for in terms of the band gaps discussed in Sec. III. The vector $\boldsymbol{\tau}$ is a reciprocal lattice vector associated with the *magnetic* symmetry. The important feature of this equation is the wave-vector dependence coming from the transformation coefficients $u_\mathbf{q}$ and $v_\mathbf{q}$, so that the probability of the transition $\mathbf{k}\to\mathbf{k}'$ will be proportional to the quantity $(u_\mathbf{q}+v_\mathbf{q})^2=(A_\mathbf{q}-B_\mathbf{q})/E(\mathbf{q})$, where $\mathbf{k}-\mathbf{k}'=\mathbf{q}+\boldsymbol{\tau}$. For wave vectors near zero, this quantity is proportional to q, resulting in a T^5 contribution to the resistivity from normal processes.[34] For wave vectors near $\mathbf{q}_0$, the quantity $(u_\mathbf{q}+v_\mathbf{q})^2$ approaches the large constant value $(8SJ_1/\omega_A)^{1/2}$. As a result, the thermally-excited magnons with wave vectors near $\mathbf{q}_0$ make the largest contribution to the low-temperature resistivity. Thus the critical nature of the assumption of cubic symmetry for the exchange constants is seen, since it is this assumption which results in the zero in the energy at the points $\mathbf{q}_0$.

Spin-Disorder Resistivity

Using the variational method in the form described by Ziman,[27] and assuming a spherical Fermi surface, we obtain the following expression for the electrical resistivity[30]:

$$\rho=C\int_0^{2k_f}\frac{d^3K(\mathbf{K}\cdot\hat{E})^2(A_\mathbf{q}-B_\mathbf{q})}{K(1-e^{-z})(e^z-1)}, \tag{13}$$

where

$$\mathbf{K}=\mathbf{k}-\mathbf{k}'=\mathbf{q}\pm\boldsymbol{\tau},\qquad z=\hbar\omega_\mathbf{q}/k_BT,$$

and

$$C=9NSG^2/8e^2k_BTk_F^4\hbar v_F^2.$$

This equation contains contributions from both normal and umklapp processes, and is also capable of giving anisotropy in the resistivity through the factor $(\mathbf{K}\cdot\hat{E})^2$. For temperatures small compared to T_N, the principal contributions to the integral occur for values of $\mathbf{q}$ lying within spheres of radius $q_m=k_BT/4SJ_1a$, about the points $\mathbf{q}=0$ and $\mathbf{q}=\mathbf{q}_0$. In $\mathbf{K}$ space, there are a large number of such spheres centered about the points $\boldsymbol{\tau}$ and $\boldsymbol{\tau}+\mathbf{q}_0$. This is a result of the fact that there are a large number of reciprocal lattice vectors $\boldsymbol{\tau}$ with magnitude less than $2k_F$. Thus umklapp processes play the dominant role, since they are more heavily weighted because of the large momentum transfer $\mathbf{K}$. Using the

[34] A. A. Berdyshev and I. N. Vlasov, Phys. Metals Metallog. (USSR) **10**, 132 (1960).

approximation $T \ll T_N$, the contributions from both normal and umklapp processes have been calculated for the a and c directions,[30] and the result is shown in Fig. 4. The normal and umklapp processes associated with wave vectors near $\mathbf{q}=0$ make contributions proportional to T^5 and T^4, respectively. The largest contribution, proportional to T^2, comes from normal and umklapp processes involving wave vectors near $\mathbf{q}_0$.

It should be noted that the magnitude of the spin-disorder resistivity depends critically on the magnitude of the exchange constants J_1 and $4J_2-J_1$, as well as on the magnitude of k_F. Further, since we have neglected the effect of a finite energy gap in the spin-wave spectrum due to the presence of an anisotropy field, a close agreement between the experimental and theoretical temperature dependences should not be expected. The anisotropy of the resistivity is, however, a property of the geometry associated with umklapp scattering processes, so that the qualitative result $\rho_a > \rho_c$ would be likely to remain in a more detailed calculation. We can see from Fig. 4 that the predicted anisotropy of the spin-disorder resistivity is in qualitative agreement with the experimental measurements.

V. ANISOTROPY OF THE SPIN-DISORDER RESISTIVITY, QUASIELASTIC THEORY

We shall now examine the effects on the resistivity of temperature-dependent spin correlations, using the quasielastic approximation, in order to relate the anisotropy of the resistivity observed just below T_N to the anisotropy of the spin correlations. The validity of the quasielastic approximation in the high-temperature region has been examined by deGennes and Friedel.[9] Their results indicate that the analysis presented here should be qualitatively valid for temperatures $T > 0.7T_N$.

Using the interaction (1), and taking the ensemble average over all states of the spin system, the square of the matrix element for transitions between conduction electron states $\mathbf{k}$ and $\mathbf{k}'$ can be written in the form

$$|\langle \mathbf{k}' \mid H \mid \mathbf{k}\rangle|^2 = G^2 \sum_{nm} \exp[i\mathbf{K}\cdot(\mathbf{R}_n-\mathbf{R}_m)]\langle \mathbf{S}_m\cdot\mathbf{S}_n\rangle_T, \tag{14}$$

where $\mathbf{K}=\mathbf{k}-\mathbf{k}'$, and the ensemble average is denoted by $\langle\cdots\rangle_T$. Defining the pair correlation function $g(\mathbf{R}_n)$ by

$$g(\mathbf{R}_n) = \langle \delta\mathbf{S}_0\cdot\delta\mathbf{S}_n\rangle_T = \langle \mathbf{S}_0\cdot\mathbf{S}_n\rangle_T - \langle \mathbf{S}_0\rangle_T\cdot\langle \mathbf{S}_n\rangle_T, \tag{15}$$

where $\delta\mathbf{S}_n=\mathbf{S}_n-\langle \mathbf{S}_n\rangle_T$, and $\mathbf{S}_0$ is a spin at $\mathbf{R}=0$, we can rewrite Eq. (14) in the form

$$|\langle \mathbf{k}' \mid H \mid \mathbf{k}\rangle|^2 = G^2N \sum_n \exp(i\mathbf{K}\cdot R_n) \times[g(\mathbf{R}_n)+\langle \mathbf{S}_m\rangle\cdot\langle \mathbf{S}_n\rangle_T]. \tag{16}$$

The second term in the square brackets describes the interaction between the conduction electrons and the long-range order of the spin system. This interaction has already been accounted for in terms of the band gaps discussed in Sec. III. Thus the spin-disorder resistivity is completely determined by the pair correlation function $g(\mathbf{R}_n)$, which is a measure of the correlations between the fluctuations of the spins. We also see from Eq. (15) that the function $g(\mathbf{R}_n)$ is a measure of the excess of short-range order over long-range order, since for neighboring spins $\mathbf{S}_i$ and $\mathbf{S}_j$, the short-range order parameter is usually defined as $\langle \mathbf{S}_i\cdot\mathbf{S}_j\rangle_T$.

Using the variational solution[27] for the electrical resistivity in the presence of elastic scattering, the following expression for the electrical resistivity is obtained[30]:

$$\rho_E = G^2NB \sum_n g(\mathbf{R}_n) f_E(\mathbf{R}_n), \tag{17}$$

where

$$f_E(\mathbf{R}_n) = \int_0^{2k_f} \frac{(\mathbf{K}\cdot\hat{E})^2 \cos(\mathbf{K}\cdot\mathbf{R}_n)\, d^3K}{K}, \tag{18}$$

and $B=9/16\hbar e^2 v_F^2 k_F^4$. Denoting the average resistivity by $\bar{\rho}=\frac{1}{3}(\rho_x+\rho_y+\rho_z)$, and the anisotropy of the resistivity by $\Delta\rho=\rho_x-\rho_z$, we find by performing the integration (18)

$$\bar{\rho} = A \sum_n L(x_n) g(\mathbf{R}_n),$$

$$L(x) = \tfrac{1}{3}(1/x^4)[-x^2\cos x + 2x\sin x - 2(1-\cos x)], \tag{19}$$

and

$$\Delta\rho = A \sum_n G(x_n) g(R_n)[\cos^2(\hat{R}_n\cdot\hat{\imath}) - \cos^2(\hat{R}_n\cdot\hat{k})],$$

$$G(x) = (1/x^4)[-x^2\cos x + 5x\sin x - 8(1-\cos x)], \tag{20}$$

where $x_n = 2k_F R_n$. The quantity A is given by $A = 36\pi NG^2/\hbar e^2 v_F^2$, and we note that $L(0)=\frac{1}{12}$, and $G(0)=0$. In the absence of pair correlations, the anisotropy is zero, and the expression for average resistivity reduces to the standard result[9] $\rho_0 = \frac{1}{12}A\langle \delta S_0^2\rangle$, where $\langle \delta S_0^2\rangle = S(S+1) - \langle S\rangle^2$.

The most significant feature of Eqs. (19) and (20) is the property that highly anisotropic spin correlations can cause a fractional anisotropy $\Delta\rho/\rho_0$ which is considerably larger than the fractional change in the average resistivity $(\bar{\rho}-\rho_0)/\rho_0$. Considering nearest-neighbor spin correlations in the AuMn lattice ($k_F = 1.42\pi/a$), we find that anisotropic correlations can cause a fractional anisotropy of up to 58% of the fractional spin correlation $|\langle \delta\mathbf{S}_0\cdot\delta\mathbf{S}_1\rangle|/\langle \delta S_0^2\rangle$, while the maximum possible change in the average resistivity is about half this amount. Thus it is possible to attribute the rapid buildup of anisotropy in the resistivity (Fig. 4) as the temperature is reduced below T_N to the buildup of anisotropic spin correlations associated with the planar magnetic ordering.

In the presence of large numbers of spin-wave excitations, the precise form of the correlation function may be quite complex. Close to the Néel temperature, however, large scale fluctuations occur in the spin system

with spin correlations extending over considerable distances and taking a form characteristic of the stable magnetic structure.[35] Thus for temperatures close to T_N, a possible correlation function would be

$$g(\mathbf{R}_n)=\gamma(R)\cos(\mathbf{Q}\cdot\mathbf{R}_n), \tag{21}$$

where $\mathbf{Q}$ has magnitude π/a and is directed along one of the three axes, and $\gamma(R)$ is an envelope function which becomes small for large R. In the paramagnetic region, the vector $\mathbf{Q}$ could be directed with equal probability along any one of the three crystallographic axes. At temperatures below T_N, where a c axis is defined, the spin correlations can be assumed to have a tetragonal form which becomes increasingly pronounced with decreasing temperature. The behavior shown in Fig. 4 can be accounted for on this basis if we assume that the polarization $\mathbf{Q}=(0, 0, 1)\pi/a$ becomes increasingly favorable with decreasing temperature. This is equivalent to assuming that the short-range order has the same planar form as the long-range order. Using Eq. (21) with the substitution

$$\mathbf{Q}=(0, 0, 1)\pi/a,$$

we find

$$\frac{\Delta\rho}{\rho}\approx 0.58\frac{|\langle\delta\mathbf{S}_0\cdot\delta\mathbf{S}_1\rangle_T|}{\langle\delta S_0^2\rangle_T}-0.29\frac{|\langle\delta\mathbf{S}_0\cdot\delta\mathbf{S}_2\rangle_T|}{\langle\delta S_0^2\rangle_T}. \tag{22}$$

Here $\mathbf{S}_1$ and $\mathbf{S}_2$ are spins in the first- and second-neighbor shells to the spin $\mathbf{S}_0$. The contribution to Eq. (22) from correlations with spins in the third- and fourth-neighbor shells is zero, and the contributions are relatively small from correlations with spins beyond the fourth-neighbor shell. The contributions of first- and second-neighbor correlations to the quantity $(\bar{\rho}-\rho_0)/\rho_0$ are less than 10% of the fractional spin correlations. Thus planar spin correlations have the effect of raising the transport cross section measured in the x direction and lowering the transport cross section measured in the z direction, leaving the resistivity averaged over direction relatively unchanged. This is consistent with the earlier conclusion that the spin-disorder resistivity is approximately temperature-independent in the paramagnetic region.

VI. DISCUSSION

The major approximation we have made in discussing the spin-disorder resistivity of the AuMn compound has been the use of a one-band, free-electron model in which the effects of *s-d* interband transitions were neglected. The justification for the use of this model was based on the conclusion that the *d*-electron contribution to the Fermi-level density of states is a relatively small percentage of the total, and on the observation that a good order of magnitude estimate of the lattice resistivity can be obtained using the same model. We have found that the magnitude of the low-temperature spin-disorder resistivity can be explained using spin-wave theory, provided that the effects of umklapp processes and of low-energy spin-wave modes with wave vectors near $\mathbf{q}=\pm(1, 0, 0)\pi/a$ and $\mathbf{q}=\pm(0, 1, 0)\pi/a$ are included. However, the magnitude of the low-temperature resistivity calculated using spin-wave theory was found to depend primarily on the excitation of these large-q spin-wave modes, which would only occur if the exchange constant J_{ij} between Mn spins had a symmetry close to cubic. We have assumed here that the tetragonal distortion and the presence of the planar magnetic ordering have a negligible effect on the symmetry of the exchange constant.

We have treated the effects on the resistivity of spin correlations using a quasielastic approximation, and have found that the correlation of the spin fluctuations is related in a very simple and direct way to the anisotropy of the spin-disorder resistivity. The most important result of this theory is that strongly anisotropic spin correlations can cause a significant anisotropy in the spin-disorder resistivity, while the effect on the resistivity averaged over direction is usually less significant. The anisotropy of the spin-disorder resistivity of AuMn in the temperature range $0.7<T<T_N$ can thus be qualitatively understood in terms of anisotropic spin correlations, provided that the fractional spin correlation $|\langle\delta\mathbf{S}_0\cdot\delta\mathbf{S}_n\rangle|/\langle\delta S_0^2\rangle$ is large for near-neighbor spins. This calculation can also be used for interpreting the resistivity in the paramagnetic regions of noncubic metals such as the heavy rare earths, in which anisotropic spin correlations could persist to quite high temperatures. The presence of anisotropic spin correlations would provide a possible mechanism for explaining the large *temperature-dependent* fractional anisotropy $(\rho_a-\rho_c)/\bar{\rho}$ observed in the paramagnetic regions of the rare earths Tb, Dy, Ho, and Er.[36]

ACKNOWLEDGMENTS

My gratitude is extended to Professor A. M. Portis for the critical guidance he has provided throughout this work. I am indebted to Professor S. F. Ravitz for his many helpful suggestions concerning the sample preparation. Thanks are also due to Dr. L. B. Welsh for assistance in the sample preparation. Helpful discussions with Professor J. W. Garland and Dr. B. Caroli are gratefully acknowledged. I am also grateful to J. F. Siebert for checking several calculations. During the sample preparation this research benefited from the partial support of the National Science Foundation.

[35] L. Van Hove, Phys. Rev. **95**, 1374 (1954); M. J. Cooper and R. Nathans, J. Appl. Phys. **37**, 1041 (1966).

[36] P. M. Hall, S. Legvold, and F. J. Spedding, Phys. Rev. **117**, 971 (1960); R. W. Green, S. Legvold, and F. J. Spedding, *ibid.* **122**, 827 (1961); D. L. Strandburg, S. Legvold, and F. H. Spedding, *ibid.* **127**, 2046 (1962); D. E. Hegland, S. Legvold, and F. H. Spedding *ibid.* **131**, 158 (1963).